Journal of Hazardous Materials 182 (2010) 557–562

Contents lists available at ScienceDirect

Journal of Hazardous Materials

journal homepage: www.elsevier.com/locate/jhazmat

Preparation and properties of visible light responsive $ZrTiO_4/Bi_2O_3$ photocatalysts for 4-chlorophenol decomposition

Bernaurdshaw Neppolian[a,1], Youngae Kim[a], Muthupandian Ashokkumar[c], Hiromi Yamashita[b], Heechul Choi[a,*]

[a] Department of Environmental Science and Engineering, Gwangju Institute of Science and Technology (GIST), 261 Cheomdam-gwagiro (Oryong-dong), Buk-gu, Gwangju 500-712, South Korea
[b] Division of Material and Manufacturing Science, Graduate School of Engineering, Osaka University, Osaka, Japan
[c] School of Chemistry, University of Melbourne, Parkville, Melbourne, Victoria 3010, Australia

ARTICLE INFO

Article history:
Received 22 January 2010
Received in revised form 16 June 2010
Accepted 16 June 2010
Available online 23 June 2010

Keywords:
TiO_2
$ZrTiO_4/Bi_2O_3$ photocatalysts
Hydrothermal
Ultrasonication
4-Chlorophenol

ABSTRACT

In this work, visible light responsive (VLR) $ZrTiO_4/Bi_2O_3$ photocatalysts were successfully synthesized by a hydrothermal method. The prepared $ZrTiO_4/Bi_2O_3$ photocatalysts were characterized by X-ray diffraction studies (XRD), X-ray photoelectron spectroscopy (XPS), diffuse reflectance spectroscopy (DRS), photoluminescence (PL) and transmission electron microscopy (TEM) analyses. DRS results revealed that the extent of light absorption towards the visible region of the spectrum increased with an increase in the calcination temperature of the catalysts up to 450 °C and then started to decrease. The decrease in absorption at high temperatures was mainly due to the formation of polycrystalline $ZrTiO_4/Bi_2O_3$ from the tetragonal Bi_2O_3 pure oxide particles. All the metals present in the $ZrTiO_4/Bi_2O_3$ composite nano-particles also exhibited corresponding oxide states. Particle sizes of about 7 nm were obtained during this combined method of preparation, especially with the catalysts calcined at 450 °C. The photocatalytic activity of the catalysts was measured using 4-chlorophenol as a model pollutant for these environmental remediation studies. Among the catalysts calcined at different temperatures, the samples calcined at 450 °C showed the most remarkable degradation of 4-chlorophenol, higher than not only the other calcined catalysts but also the commercially available Degussa P-25. This is due to the formation of smaller particle sizes, a higher surface area and stronger absorption in the visible light irradiation for these catalysts calcined at 450 °C. Thus, such new VLR photocatalysts can be expected to work effectively under visible light regions as an applicable alternative photocatalyst for commercial scale use.

1. Introduction

In recent years, nano-scale semiconductor materials have been the focus of much research, especially in the development of environmental remediation processes using nano-size TiO_2 photocatalysts [1–11]. TiO_2 is generally considered the most promising and is widely used in heterogeneous photocatalysis [1–11]. However, nano-size TiO_2 has a relatively large band gap of 3.2 eV, so that it is able to work more efficiently under the high energy of UV light irradiation and not visible light [2]. Moreover, TiO_2 makes use of only 5% of the UV light from the solar beams that reach the earth's surface [12,13]. In order to utilize the maximum energy of the solar spectrum, the development of TiO_2 photocatalysts which can operate efficiently under both UV and visible light irradiation will be vital. In fact, visible light responsive (VLR) narrow band gap semiconductor photocatalysts in the form of a composite or mixed oxide catalysts and referred to as the second-generation TiO_2 photocatalysts are presently under development [13,26].

Among the various newly developed narrow band gap VLR photocatalysts (CdS, CdSe, ZnS, etc.), Bi_2O_3 semiconductor has been widely used due to its stability and small band gap (2.8 eV) [14–16] which is sufficient to absorb visible light of around 450 nm. However, with Bi_2O_3 semiconductors, there are more chances for the recombination of photo-formed electrons and holes due to the small band gap. In order to improve the quantum efficiency of both TiO_2 and Bi_2O_3 under visible light irradiation, Bi_2O_3 has been synthesized as a binary metal oxide catalyst (TiO_2–Bi_2O_3) with different weight ratios of Bi and Ti and then applied for the degradation of pollutants [14–16]. In this binary system, a slow shift of the absorption spectra of the catalysts towards the visible region is observed in accordance with the amount of Bi_2O_3 [14,15]. It is evident that Bi_2O_3 effectively works as a sensitizer and works to

* Corresponding author. Tel.: +82 62 970 2441; fax: +82 62 970 2434.
E-mail addresses: hcchoi@gist.ac.kr, hcchoi@kjist.ac.kr (H. Choi).
[1] Present address: Particulate Fluids Processing Centre, School of Chemistry, University of Melbourne, Parkville, Melbourne, Victoria 3010, Australia.

0304-3894/$ – see front matter © 2010 Elsevier B.V. All rights reserved.
doi:10.1016/j.jhazmat.2010.06.069

harvest sunlight more efficiently than TiO_2 alone. Bian et al. [14] and Bessekhouad et al. [17] have also reported the inter-particle electron transfer from the conduction band of Bi_2O_3 to the conduction band of TiO_2, i.e., that Bi_2O_3 operates as a sensitizer. This process, thus, enhances the charge separation and increases the quantum efficiency.

In a previous study, we have observed that small amounts of ZrO_2 are able to control all the physico-chemical properties of TiO_2, which in turn can increase the efficiency of TiO_2 photocatalysis. The particle size is especially well-controlled by ZrO_2 in binary oxide catalysts [18]. Some studies have also explored the application of ultrasound for the preparation of nano-particles, especially TiO_2 [19–28]. During ultrasonic irradiation, ultrasonic waves consisting of compression and rarefraction cycles produce cavitation bubbles in a liquid. After several compression/rarefaction cycles, the cavitation bubbles collapse violently and adiabatically at extremely high temperatures of up to 5000 °C and pressures of about 500 atm [19,20]. Such extreme temperatures and pressures within a small reactor can induce many changes in the morphology of the TiO_2 nano-particles during the preparation process. Ultrasonic irradiation is usually favorable for mass transfer during the preparation of metal oxide particles. This would alter the kinetics of the reactions during nano-material preparation [19,20].

In this study, we report on the preparation of Bi_2O_3 along with TiO_2 and ZrO_2 as a combination of three mixed-oxide photocatalysts by employing an ultrasonic-assisted hydrothermal method. Characterization studies of the mixed oxide catalysts and their effect on the visible light reactivity for the degradation of 4-chlorophenol (4-CP) were also carried out and are presented here.

2. Experimental

2.1. Materials

Titanium(IV) isopropoxide (TTIP), zirconium(IV) isopropoxide isopropanol complex, bismuth nitrate pentahydrate, polyvinylpyrrolidine, 4-chlorophenol (4-CP) and 2-propanol were purchased from the Aldrich Company and were used without further purification. Deionized (DI) water was used for the preparation of all the catalysts as well as to dilute the 4-CP solution.

2.2. Preparation of the $ZrTiO_4/Bi_2O_3$ visible light photocatalysts

$ZrTiO_4/Bi_2O_3$ nanoparticles were synthesized by an ultrasonic-assisted hydrothermal method in which bismuth nitrate pentahydrate, titanium(IV) isopropoxide (TTIP) and a zirconium(IV) isopropoxide isopropanol complex were used as precursors for Bi_2O_3, TiO_2 and ZrO_2, respectively. Bismuth nitrate pentahydrate of 3.3 g was dissolved in 30 mL of 1.12 M HNO_3 acid while 1.0 g of polyvinyl pyrolidone (PVP) was added to the bismuth nitrate hydrate solution and kept for 30 min under stirring [29]. TTIP and zirconium(IV) isopropoxide isopropanol (TiO_2/ZrO_2 = 2:1) was separately mixed (in 100 mL of HNO_3 solution), as reported earlier [18], and kept for 30 min under stirring. NaOH of 0.9 g (0.2 M NaOH) was added to the TTIP and zirconium(IV) isopropoxide isopropanol solution and the solution pH rose to 13. Bismuth nitrate pentahydrate solution with PVP was added drop wise into the TTIP and zirconium(IV) isopropoxide isopropanol solution under vigorous stirring and kept for another 15 min. The mixture was then placed on an ultrasonicator (40 kHz, Branson 8510, USA) for 1 h. After the ultrasonicator bath, the colloidal solution was replaced in an autoclave (65% of its total volume) and sealed tightly. The autoclave was placed on a furnace and slowly heated up to 170 °C (2 °C/min) and kept for another 15 h under the same temperature. The product was then allowed to cool to room temperature. Finally, the mixed oxide catalyst was washed many times with distilled water, then with ethanol to remove all of the PVP present in the solution and dried at 120 °C for 12 h. The dried mixed oxide catalysts were then calcined at various temperatures (400–550 °C) with an electric furnace (2 °C/min) and, finally, ground to fine powder using a pestle and mortar.

2.3. Characterizations

The crystalline structure of the $ZrTiO_4/Bi_2O_3$ particles were investigated by X-ray powder diffraction analysis (XRD, Rigaku RDA-ϒA X-ray diffractometer, D/MAX Ultima III, Japan) using Cu Kα radiation with a Ni filter. The morphology and size distribution of the photocatalysts were recorded by transmission electron microscopy (TEM, JEOL, JEM 2100, Japan). Before analyses, the samples were placed on the surface of copper grids and dried under ambient conditions. The N_2 BET surface area, pore-volume, pore-size distribution, porosity, and pore diameter of the photocatalysts were determined by a BET analyzer (Micromeritics, ASAP 2020, USA). The photoluminescence spectra were recorded at 300 K using a He–Cd laser (λ = 325 nm) as the excitation source (Optron, South Korea). The UV–Vis reflectance of the catalysts was measured by diffuse reflectance spectroscopy using a Hitachi U3501 (Integrating Sphere) instrument. Band gap values of the prepared catalysts were determined from plots of the modified Kubelka–Munk function $[F(R\infty)E]^{1/2}$ versus the energy of the excitation light [29,30]. ICP-MS was used to determine the actual wt.% of the Bi_2O_3, TiO_2 and ZrO_2 present in the mixed oxide catalysts (Agilent 7500ce, TCP-MS, USA). The XPS spectra of the photocatalysts were measured at 295 K with a V.G. Scientific ESCASCOPE photoelectron spectrometer using Mg Kα radiation.

2.4. Photocatalytic activity measurements

The photocatalytic activity was evaluated by the reaction rates for the oxidative degradation of 4-chlorophenol (4-CP). The photocatalyst (300 mg) was suspended in a quartz cell with an aqueous solution of 4-CP (1.25×10^{-4} M, 200 mL). Prior to UV light irradiation, the suspension was stirred for 30 min in oxygen atmosphere under dark conditions. The sample was then irradiated at 24 °C using UV light (transmitting range, λ 200–800 nm) from a 300 W Xe Arc lamp (Oriel Lamp, Model 66984, USA) under continuous stirring in oxygen atmosphere. A 410 cut-off filter was used to block the UV light and allow only visible light to go through. At periodic intervals, up to 5 mL aliquots were taken from the system and filtered through a Millipore filter to remove the TiO_2 particles. The percentage of degradation was then analyzed by a 144 HPLC (Shimadzu LC-10 AT VP system with a Shimadzu SPD-M10 145A VP photodiode array detector with a Phenomenex reversed phase 146 column).

3. Results and discussion

3.1. Physicochemical characteristic studies

The wt.% of the pure photocatalysts (Bi_2O_3, TiO_2 and ZrO_2) present in the mixed oxide catalysts, $ZrTiO_4/Bi_2O_3$, was verified by ICP-MS, SEM-EDS and TEM-EDS analyses and the results are presented in Table 1. The ratio between TiO_2 and ZrO_2 was 1:0.5 which was similar to the theoretical value, and the ratio between Bi_2O_3 and TiO_2/ZrO_2 was around 3:1 as per values obtained from ICP-MS, SEM-EDS and TEM-EDS analyses (Table 1).

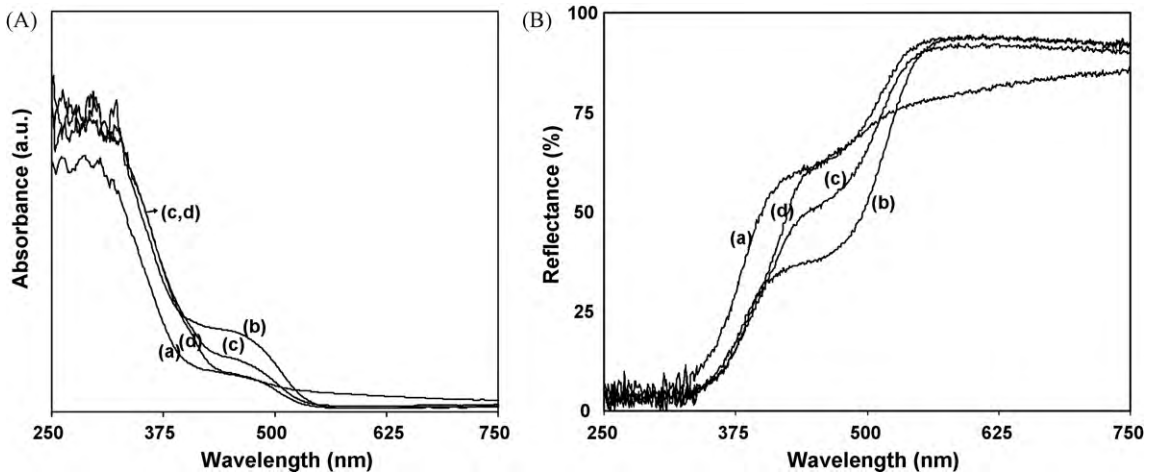

Fig. 1. (A) Absorbance spectra of $ZrTiO_4/Bi_2O_3$ photocatalysts calcined at different temperatures: (a) 400 °C, (b) 450 °C, (c) 500 °C, and (d) 550 °C. (B) Corresponding diffuse reflectance spectra of $ZrTiO_4/Bi_2O_3$ photocatalysts calcined at different temperatures: (a) 400 °C, (b) 450 °C, (c) 500 °C, and (d) 550 °C.

Table 1
The ICP-MS, SEM-EDS and TEM-EDS values of wt.% ratio of pure TiO_2, ZrO_2 and Bi_2O_3 present in $ZrTiO_4/Bi_2O_3$ photocatalysts calcined at 450 °C.

Methods	wt.% of Bi	wt.% of Ti	wt.% of Zr	Bi:(Ti/Zr)
ICP-MS	60.87	12.67	6.25	3.22:1
SEM-EDS	66.50	13.85	7.81	3.07:1
TEM-EDS	65.17	12.32	7.63	3.26:1

3.2. Absorption spectroscopy

The diffuse reflectance spectra and its corresponding absorbance spectra of $ZrTiO_4/Bi_2O_3$ calcined at different temperatures from 400 to 550 °C are shown in Fig. 1. A shift towards longer wavelength regions of light is observed although it is not smooth and unlike the smooth shift when Fe is doped into TiO_2 by an ion-implantation method, an advanced technique for the implantation of metal ions into TiO_2 [31]. However, a new absorption band was formed at 450 nm due to the presence of Bi ions. The intensity of the impurity energy level increased with an increase in the calcination temperature and a maximum was observed with the catalysts calcined at 450 °C and then decreased. This absorption shift is similar to the chemical doping of metal (transition metals) on TiO_2 [31]. These results suggest that there is no strong chemical interaction between Bi_2O_3 and the TiO_2–ZrO_2 photocatalysts. On the other hand, a small red shift was observed with the catalysts calcined at 500 and 550 °C, as shown in Fig. 1(A), which revealed that to some extent, chemical interactions exist between the mixed oxides at higher calcination temperatures. Bian et al. [14] have reported about 1–5 wt.% Bi_2O_3 on the TiO_2 photocatalysts in which the extent of absorption towards the visible light region was in direct proportion to the amount of Bi_2O_3 loading. Furthermore, the absorption region of the catalysts extended to ~560 nm so that Bi_2O_3 could efficiently absorb visible light and transfer the photo-formed electrons to the conduction band of TiO_2. The band gap calculated was 2.88 eV for $ZrTiO_4/Bi_2O_3$ of the 450 °C calcined catalysts.

3.3. XRD

The phase structure and crystallinity of $ZrTiO_4/Bi_2O_3$ were examined by XRD analysis. The XRD patterns of $ZrTiO_4/Bi_2O_3$ calcined from 400 to 550 °C are shown in Fig. 2. For the catalysts calcined at 400 and 450 °C, the XRD patterns confirm the formation of tetragonal Bi_2O_3 similar to pure Bi_2O_3 (JCPDS FILE 78-1793). There were no characteristic XRD patterns for TiO_2 or ZrO_2. Generally, for ZrO_2 and TiO_2 binary oxide catalysts, the XRD patterns of both ZrO_2 and TiO_2 overlap as we have observed in earlier findings with TiO_2–ZrO_2 [18]. Furthermore, the amount of both oxides (TiO_2–ZrO_2) was less than Bi_2O_3. The catalysts calcined at 500 and 550 °C both possessed the tetragonal phase of pure Bi_2O_3 (JCPDS FILE 78-1793) and polycrystalline tetragonal phase of $Bi_4Ti_3O_{12}$ (JCPDS file 47-0398) [15,32]. These observations imply that, with the catalysts calcined at 500 and 550 °C, Bi_2O_3 reacted with TiO_2 and formed polycrystalline $Bi_4Ti_3O_{12}$ along with pure Bi_2O_3, however, the proportion of pure Bi_2O_3 gradually decreased with an increase in the calcination temperature. It was also revealed that during hydrothermal synthesis at 170 °C for 15 h, no chemical interaction occurred between the Bi_2O_3 and TiO_2 oxides, and that calcination at high temperatures only induced chemical interactions among the oxides. With the catalysts calcined at 550 °C, the $Bi_4Ti_3O_{12}$ peak was almost equal to that of pure Bi_2O_3, whereas, with the 500 °C calcined catalysts, a very small peak for $Bi_4Ti_3O_{12}$ was observed. The DRS and absorbance results also support the results obtained from XRD, i.e., for both the 500 and 550 °C calcined catalysts, the red shift is only slightly smooth, a characteristic normally attributed to chemically bonded catalysts (Fig. 1(A)) [31]. Similarly, Zhou et al. [15] have also reported the same type of spectra for Bi_2O_3–TiO_2 photocatalysts. Among the four

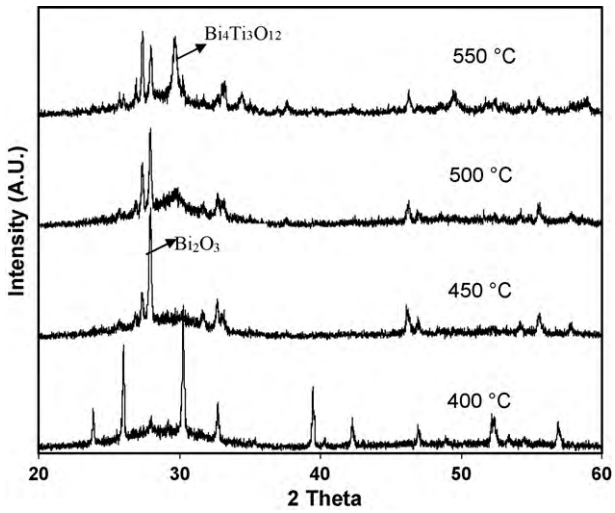

Fig. 2. XRD patterns of $ZrTiO_4/Bi_2O_3$ photocatalysts calcined at different temperatures: (a) 400 °C, (b) 450 °C, (c) 500 °C, and (d) 550 °C.

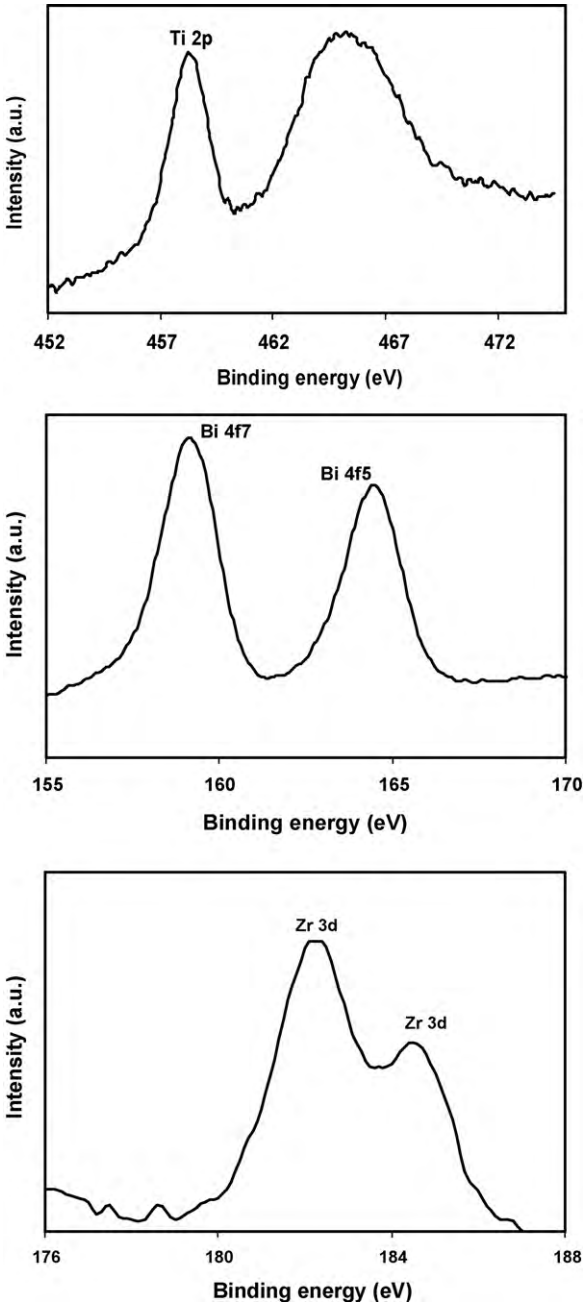

Fig. 3. XPS spectra of $ZrTiO_4/Bi_2O_3$ photocatalysts calcined at 450 °C.

diffraction patterns of $ZrTiO_4/Bi_2O_3$, the crystallinity of Bi_2O_3 was higher with the catalysts calcined at 450 °C than any of the other catalysts.

3.4. XPS

The XPS spectra of $ZrTiO_4/Bi_2O_3$ were analyzed to obtain information on the binding energy of all of the three oxides in order to determine the surface chemical states of Bi, Ti and Zr in the mixed oxide catalysts. A peak was observed for the binding energy of Bi composed of two signals at binding energies of 159.1 and 164.4 eV in Bi_{4f7} and Bi_{4fd}, respectively (Fig. 3). The binding energy of the Bi_2O_3 values shifted slightly to the positive by ~0.4 eV in comparison to pure Bi_2O_3, as reported by Bian et al. [14]. The shifting of the binding energies values to slightly higher values can be attributed to the smaller relaxation energy of the highly dispersed Bi_2O_3 in the

Table 2
Physico-chemical characterization of $ZrTiO_4/Bi_2O_3$ prepared by ultrasound-assisted hydrothermal method.

Calcinations temp. (3 h) (°C)	Particle size TEM (nm)	Surface area (m^2/g)	Aggregated pore-size (nm)	Pore-volume (cm^3/g)
400	5	54	14.1	0.190
450	7	48	17.0	0.200
500	11	30	18.3	0.135
550	15	20	14.2	0.171

$ZrTiO_4/Bi_2O_3$ mixed oxide catalysts [13]. However, no such shifting of the binding energy value was observed for TiO_2. The binding energy value of TiO_2 was obtained at 458.4 eV which is the same as the pure TiO_2 photocatalysts. Thus, TiO_2 was present in its pure state with the $ZrTiO_4/Bi_2O_3$ mixed oxide catalysts. The XPS of Zr in the $ZrTiO_4/Bi_2O_3$ mixed oxide catalysts is also shown in Fig. 3 while the two signals at binding energies 182.5 and 184.5 eV correspond to the Zr_{3d} peaks similar to pure ZrO_2 [33]. These results reveal that Bi, Ti and Zr exist in its pure oxide form in the $ZrTiO_4/Bi_2O_3$ mixed oxide catalysts calcined at 450 °C.

3.5. BET

The BET surface area, pore-volume and pore-size of the $ZrTiO_4/Bi_2O_3$ photocatalysts calcined at different temperatures from 400 to 550 °C were determined using a BET instrument and the results are presented in Table 2. The surface area of the catalysts is observed to noticeably decrease from 54 to 20 m^2/g with an increase in the calcination temperature from 400 to 550 °C. When the calcination temperature increased, well crystallined particles of larger sizes were formed. Thus, it was observed that the formation of larger particles at higher temperatures was responsible for the reduction in the surface area of $ZrTiO_4/Bi_2O_3$. However, the aggregated pore-size was gradually enhanced with the calcination temperature up to 500 °C and then decreased, while at the same time, an enhanced reduction in the pore-volume occurred after 450 °C (Table 2).

3.6. TEM

The shape and size of the $ZrTiO_4/Bi_2O_3$ particles were examined by a TEM instrument and Fig. 4 shows the TEM images of $ZrTiO_4/Bi_2O_3$ calcined at 450 °C as the representative catalyst among the other $ZrTiO_4/Bi_2O_3$ catalysts, most of which have spherical shape particles with an average size of 7–8 nm. Similarly, the same spherical particle shape could be retained for the other catalysts calcined at 500 and 550 °C, however, their average particle

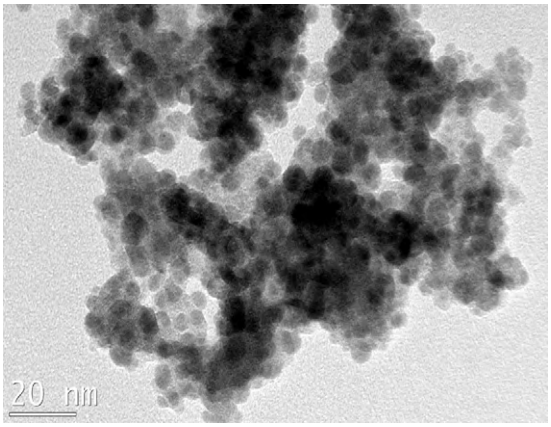

Fig. 4. TEM image of $ZrTiO_4/Bi_2O_3$ photocatalysts calcined at 450 °C.

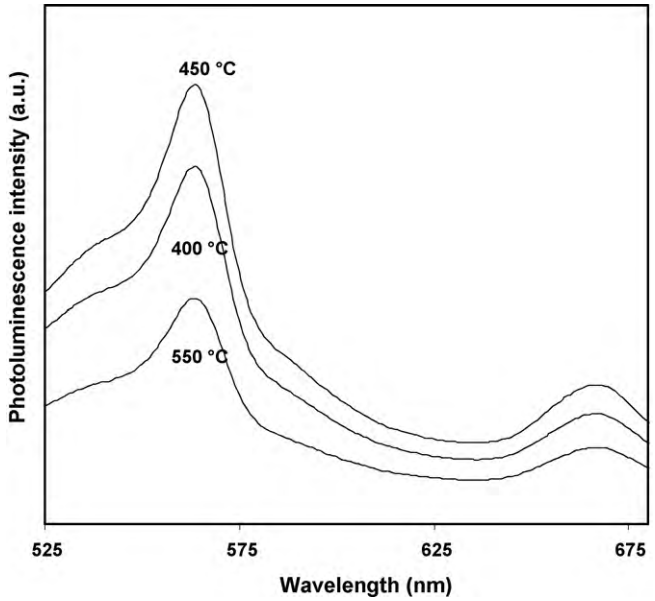

Fig. 5. Photoluminescence spectra of $ZrTiO_4/Bi_2O_3$ photocatalysts calcined at different temperatures: from 400 to 550 °C.

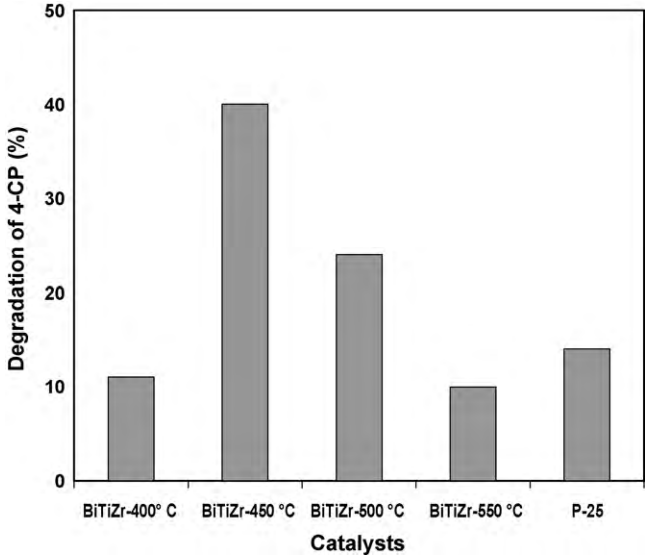

Fig. 6. Photocatalytic degradation (%, based on HPLC analysis) of 4-chlorophenol by $ZrTiO_4/Bi_2O_3$ photocatalysts calcined at different temperatures: from 400 to 550 °C in 1 h.

sizes were higher (~10–15 nm) than that of the catalysts calcined at 450 °C, as shown in Table 2.

3.7. Photoluminescence spectra

Measurements of the photoluminescence (PL) spectra of the $ZrTiO_4/Bi_2O_3$ catalysts were carried out with a 450 nm laser excitation source and the corresponding spectra of each sample are depicted in Fig. 5. The PL spectra of both the 450 and 500 °C calcined $ZrTiO_4/Bi_2O_3$ photocatalysts were very similar, whereas, the intensity of the PL spectra of the $ZrTiO_4/Bi_2O_3$ catalyst calcined at 550 °C was less than for the ones calcined at 400 °C as well as the other two calcined catalysts (450 and 500 °C), as shown in Fig. 5. Generally, the area (integrated intensity) of the PL spectra is relatively proportional to the number of photo-generated electrons and holes [18], the maximum observed with the 450 and 500 °C calcined photocatalysts. It is known that catalysts calcined at 400 °C possess mostly amorphous particles with imperfections and lattice defects in the crystal structure, leading to more recombination of the photo-generated electrons and holes when excited [18,19]. On the other hand, for the 550 °C calcined $ZrTiO_4/Bi_2O_3$, the area of the PL spectra was much less than that of the other calcined catalysts. This may be due to fact that the number of photo-generated electrons and holes was speculated to be less with the 550 °C calcined catalysts due their larger size particles (13–15 nm) and higher proportion of a tetragonal phase $Bi_4Ti_3O_{12}$ than the pure phase of Bi_2O_3. These PL spectra results further confirm and support the XRD results.

3.8. Photocatalytic activity for the degradation of 4-chlorophenol

The photocatalytic activity of the $ZrTiO_4/Bi_2O_3$ catalysts calcined at different temperatures (400–550 °C) was compared for the degradation of 4-chlorophenol (4-CP), diluted with water. Among the four different calcined catalysts, the $ZrTiO_4/Bi_2O_3$ catalyst calcined at 450 °C exhibited the highest photocatalytic activity under visible light irradiation than the other calcined catalysts including the P-25 Degussa photocatalysts, as shown in Fig. 6. Degradation of 40% for 4-CP was achieved with 1 h irradiation time for the 450 °C calcined catalysts, whereas only 24% degradation was observed for the ones calcined at 500 °C, and about 10% degradation for the 400 and 550 °C calcined catalysts. The greater degradation efficiency of the 450 °C calcined $ZrTiO_4/Bi_2O_3$ catalysts was mainly due to the larger shift of light absorption towards visible regions, as shown by the absorbance spectra (Fig. 1(A)), enabling them to absorb more light under the visible spectrum and leading to higher activity. Moreover, the crystallinity of Bi_2O_3 was very high for the 450 °C calcined catalysts, as shown by the XRD patterns (Fig. 2). In addition to crystallinity, the 500 and 550 °C catalysts possessed mixed oxides containing both pure Bi_2O_3 and $Bi_4Ti_3O_{12}$. For $Bi_4Ti_3O_{12}$, the absorption towards visible light regions was less than for the 450 °C catalysts (Fig. 1(A)) while the particle size of $ZrTiO_4/Bi_2O_3$ was larger for both the 500 and 550 °C calcined catalysts (Table 2). Zhou et al. [15] have reported that the cubic phase of $Bi_4Ti_3O_{12}$ has higher activity for the degradation of methanol than its tetragonal phase. They also state that at higher calcination temperatures, the cubic form of $Bi_4Ti_3O_{12}$ changed into a tetragonal phase which is unfavorable for visible light induced reactions. The existence of a tetragonal phase for the polycrystalline catalysts is yet another reason for the low activity of the catalysts calcined at 500 and 550 °C. These are the main factors behind the low degradation of 4-CP with these catalysts. Catalysts calcined at 400 °C were mostly amorphous which in turn suppressed the photocatalytic activity, as has been described earlier. Also, analysis of the PL spectra offers further information on the reactivity of the catalysts for the degradation of 4-CP. The PL intensity is relatively higher for the 450 and 500 °C calcined catalysts than 400 and 550 °C calcined ones, indicating that more photo-formed electrons were excited during the reaction. However, in the case of the 450 °C calcined catalysts, the recombination rate may be much less than the 500 °C calcined catalysts. For the 450 °C calcined catalysts, mostly pure Bi_2O_3 existed so that the photo-formed electrons were easily transferred to the conduction band edge of TiO_2, as has been reported by Bian et al. [14] and Bessekhouad et al. [17]. Even though the 500 °C calcined catalysts exhibited the same PL intensity as that of the 450 °C calcined catalysts, it is mostly the $Bi_4Ti_3O_{12}$ phase that exists along with pure Bi_2O_3. However, the $Bi_4Ti_3O_{12}$ tetragonal phase is unfavorable for the degradation of 4-CP, as has been described earlier. Table 2 shows the surface area of the catalysts and the catalysts calcined at 450 °C possess a surface area of 48 m^2/g, whereas, 30 m^2/g surface area was observed for the catalysts calcined at 500 °C. 38%

of the surface area decreased when the catalysts were calcined from 450 to 500 °C and this was further reflected in the photocatalytic degradation of 4-CP. However, for the 550 °C calcined catalysts, the surface area drastically decreased to 20 m^2/g and, hence, catalytic activity was much retarded, another reason for less efficient degradation of 4-CP. It is clear from the investigations and above discussions that not only is the absorption of the catalysts towards visible light regions necessary for a high efficiency in the degradation of 4-CP but also such parameters as the morphology, PL intensity, particle size, surface area and crystallinity are also equally essential to the performance. Furthermore, the catalysts prepared without hydrothermal treatment or ZrO_2 have shown around 50% less degradation of 4-CP than in the presence of ZrO_2 and the hydrothermal method. These results, thus, reveal that both ZrO_2 as well as hydrothermal treatment were also responsible for the high degradation of 4-CP. In order to confirm the stability of the catalysts, experiments were carried out 3 consecutive runs by reusing the $ZrTiO_4/Bi_2O_3$ photocatalyst. There was about 10–12% decrease on the percentage of 4-CP degradation, noted in each time. The decrease in the efficiency of the catalyst during each subsequent run might be due to the dissolution of particles during the reaction.

4. Conclusions

Visible light responsive photocatalysts $ZrTiO_4/Bi_2O_3$ were prepared by an ultrasound-assisted hydrothermal method and were proved to be highly effective for the degradation of 4-CP within a short period of time. Though the ability of the catalysts for absorption towards the visible region is the main reason for their higher activity in the visible spectrum of light, other physico-chemical characteristics, such as particle size, surface area, crystallinity, and PL characterization, were also important factors in determining their catalytic performance. Among the catalysts calcined at different temperatures, the samples calcined at 450 °C showed higher activity for the degradation of 4-CP than those calcined at higher temperatures, thus, offering the advantage of catalyst preparation at low calcination temperatures.

Acknowledgements

This research was supported by a Grant (M1050000012805-J000012810) from the Korea Ministry of Science and Technology through the National Research Laboratory Program and partially supported by Korea Science and Engineering Foundation (KOSEF).

References

[1] W. Choi, Pure and modified TiO_2 photocatalysts and their environmental applications, Catal. Surv. Asia 10 (2006) 16–28.
[2] M. Anpo, Preparation, characterization, and reactivities of highly functional titanium oxide-based photocatalysts able to operate under UV–visible light irradiation: approaches in realizing high efficiency in the use of visible light, Bull. Chem. Soc. Jpn. 77 (2004) 1427–1442.
[3] J. Peller, O. Wiest, P.V. Kamat, Synergy of combining sonolysis and photocatalysis in the degradation and mineralization of chlorinated aromatic compounds, Environ. Sci. Technol. 37 (2003) 1926–1932.
[4] J.F. Zhu, J.L. Zhang, F. Chen, M. Anpo, Preparation of high photocatalytic activity TiO_2 with a bicrystalline phase containing anatase and TiO_2 (B), Mater. Lett. 59 (2005) 3378–3381.
[5] H. Yamashita, M. Harada, A. Tanii, M. Honda, M. Takeuchi, Y. Ichihashi, M. Anpo, N. Iwamoto, N. Itoh, T. Hirao, Preparation of efficient titanium oxide photocatalysts by an ionized cluster beam (ICB) method and their photocatalytic reactivities for the purification of water, Catal. Today 63 (2000) 63–69.
[6] M.R. Ghezzar, F. Abdelmalek, M. Belhadj, N. Benderdouche, A. Addou, Enhancement of the bleaching and degradation of textile wastewaters by Gliding arc discharge plasma in the presence of TiO_2 catalyst, J. Hazard. Mater. 164 (2009) 1266–1274.
[7] F.L. Toma, G. Bertrand, S. Begin, C. Meunier, O. Barres, D. Klein, C. Coddet, Microstructure and environmental functionalities of TiO_2-supported photocatalysts obtained by suspension plasma spraying, Appl. Catal. B: Environ. 68 (2006) 74–84.
[8] M. Addamo, M. Bellardita, D. Carriazo, A.D. Paola, S. Milioto, L. Palmisano, V. Rives, Inorganic gels as precursors of TiO_2 photocatalysts prepared by low temperature microwave or thermal treatment, Appl. Catal. B: Environ. 84 (2008) 742–748.
[9] Y. Sakata, T. Yamamoto, T. Okazaki, H. Imamura, S. Tsuchiya, Generation of visible light response on the photocatalyst of a copper ion containing TiO_2, Chem. Lett. 12 (1998) 1253–1254.
[10] D. Dionysiou, A.P. Khodadoust, A.M. Kern, M.T. Suidan, I. Baudin, J.M. Laine, Continuous-mode photocatalytic degradation of chlorinated phenols and pesticides in water using a bench-scale TiO_2 rotating disk reactor, Appl. Catal. B: Environ. 24 (2000) 139–155.
[11] H. Park, H.S. Jie, B. Neppolian, K. Tsujimaru, J.-P. Ahn, D.Y. Lee, J.-K. Park, M. Anpo, Preparation of highly active TiO_2 nano-particle photocatalysts by a flame aerosol method for the complete oxidation of 2-propanol, Top. Catal. 47 (2008) 166–174.
[12] B. Neppolian, H.C. Choi, S. Sakthivel, B. Arabindoo, V. Murugesan, Solar/UV-induced photocatalytic degradation of three commercial textile dyes, J. Hazard. Mater. B89 (2002) 303–317.
[13] M. Anpo, M. Takeuchi, The design and development of highly reactive titanium oxide photocatalysts operating under visible light irradiation, J. Catal. 216 (2003) 505–516.
[14] Z.F. Bian, J. Zhu, S.H. Wang, Y. Cao, X.F. Qian, H.X. Li, Self-assembly of active Bi_2O_3/TiO_2 visible photocatalyst with ordered mesoporous structure and highly crystallized anatase, J. Phys. Chem. C 112 (2008) 6258–6262.
[15] J. Zhou, Z. Zou, A.K. Ray, X.S. Zhao, Preparation and characterization of polycrystalline bismuth titanate $Bi_{12}TiO_{20}$ and its photocatalytic properties under visible light irradiation, Ind. Eng. Chem. Res. 46 (2007) 745–749.
[16] W.F. Yao, H. Wang, X.H. Xu, X.F. Cheng, J. Huang, S.X. Shang, X.N. Yang, M. Wang, Photocatalytic property of bismuth titanate $Bi_{12}TiO_{20}$ crystals, Appl. Catal. A: Gen. 243 (2003) 185–190.
[17] Y. Bessekhouad, D. Robert, J.-V. Weber, Photocatalytic activity of CU_2O/TiO_2, Bi_2O_3/TiO_2 and $ZnMn_2O_4/TiO_2$ heterojunctions, Catal. Today 101 (2005) 315–321.
[18] B. Neppolian, Q. Wang, H. Yamashita, H. Choi, Synthesis and characterization of ZrO_2–TiO_2 binary oxide semiconductor nanoparticles: application and interparticle electron transfer process, Appl. Catal. A: Gen. 333 (2007) 264–271.
[19] B. Neppolian, Q. Wang, H. Jung, H. Choi, Ultrasonic-assisted sol–gel method of preparation of TiO_2 nano-particles: characterization, properties and 4-chlorophenol removal application, Ultrason. Sonochem. 15 (2008) 649–658.
[20] B. Neppolian, E. Celik, M. Anpo, H. Choi, Ultrasonic-assisted pH swing method for the synthesis of highly efficient TiO_2 nano-size photocatalysts, Catal. Lett. 125 (2008) 183–184.
[21] K.S. Suslick, G.J. Price, Applications of ultrasound to materials chemistry, Ann. Rev. Mater. Sci. 29 (1999) 295–326.
[22] Y. Wang, X. Tang, L. Yin, W. Huang, Y.R. Hacohen, A. Gedanken, Sonochemical synthesis of mesoporous titanium oxide with wormhole-like framework structures, Adv. Mater. 12 (2000) 1183–1186.
[23] J.C. Yu, J. Yu, W. Ho, L. Zhang, Preparation of highly photocatalytic active nano-sized TiO_2 particles via ultrasonic irradiation, Chem. Commun. (2001) 1942–1943.
[24] J.C. Yu, L. Zhang, J. Yu, Direct sonochemical preparation and characterization of highly active mesoporous TiO_2 with a bicrystalline framework, Chem. Mater. 14 (2002) 4647–4653.
[25] J.C. Yu, L. Zhang, J. Yu, Rapid synthesis of mesoporous TiO_2 with high photocatalytic activity by ultrasound-induced agglomeration, New J. Chem. 26 (2002) 416–420.
[26] W. Ho, J.C. Yu, Sonochemical synthesis and visible light photocatalytic behavior of CdSe and $CdSe/TiO_2$ nanoparticles, J. Mol. Catal. A: Chem. 247 (2006) 268–274.
[27] C.W. Oh, G.D. Lee, S.S. Park, C.S. Ju, S.S. Hong, Synthesis of nanosized TiO_2 particles via ultrasonic irradiation and their photocatalytic activity, React. Kinet. Catal. Lett. 85 (2005) 261–268.
[28] P.S. Awati, S.V. Awate, P.P. Shah, V. Ramaswamy, Photocatalytic decomposition of methylene blue using nanocrystalline anatase titania prepared by ultrasonic technique, Catal. Commun. 4 (2003) 393–400.
[29] L. Zhang, W. Wang, J. Yang, Z. Chen, W. Zhang, L. Zhou, S. Liu, Sonochemical synthesis of nanocrystallite Bi_2O_3 as a visible-light-driven photocatalyst, Appl. Catal. A: Gen. 308 (2006) 105–110.
[30] J.C. Colmenares, M.A. Aramendı, A. Marinas, J.M. Marinas, F.J. Urbano, Synthesis, characterization and photocatalytic activity of different metal-doped titania systems, Appl. Catal. A: Gen. 306 (2006) 120–127.
[31] H Yamashita, M. Harada, J. Misaka, M. Takeuchi, B. Neppolian, M. Anpo, Photocatalytic degradation of organic compounds diluted in water using visible light-responsive metal ion-implanted TiO_2 catalysts: Fe ion-implanted TiO_2, Catal. Today 84 (2003) 191–196.
[32] W.L. Liu, H.R. Xia, H. Han, X.Q. Wang, Synthesis and structure of bismuth titanate nanopowders prepared by metalorganic decomposition method, J. Mater. Sci. 40 (2005) 1827–1829.
[33] B. Wu, R. Yuan, X. Fu, Structural characterization and photocatalytic activity of hollow binary ZrO_2/TiO_2 oxide fibers, J. Solid State Chem. 182 (2009) 560–565.